Organic & Biomolecular Chemistry

Cite this: *Org. Biomol. Chem.*, 2011, **9**, 8246

www.rsc.org/obc

PAPER

Naphthalene- and perylenediimides with hydroquinones, catechols, boronic esters and imines in the core†‡

Andrea Fin,§ Irina Petkova,§ David Alonso Doval, Naomi Sakai, Eric Vauthey and Stefan Matile*

Received 3rd May 2011, Accepted 11th July 2011
DOI: 10.1039/c1ob05702b

The green-fluorescent protein of the jellyfish operates with the most powerful phenolate donors in the push–pull fluorophore. To nevertheless achieve red fluorescence with the same architecture, sea anemone and corals apply oxidative imination, a process that accounts for the chemistry of vision as well. The objective of this study was to apply these lessons from nature to one of the most compact family of panchromatic fluorophores, *i.e.* core-substituted naphthalenediimides (cNDIs). We report straightforward synthetic access to hydroxylated cNDI and cPDI cores by palladium-catalyzed cleavage of allyloxy substituents. With hydroxylated cNDIs but not cPDIs in water-containing media, excited-state intramolecular proton transfer yields a second bathochromic emission. Deprotonation of hydroquinone, catechol and boronic ester cores provides access to an impressive panchromism up to the NIR frontier at 640 nm. With cNDIs, oxidative imination gives red shifts up to 638 nm, whereas the expanded cPDIs already absorb at 754 nm upon deprotonation of hydroquinone cores. The practical usefulness of hydroquinone cNDIs is exemplified by ratiometric sensing of the purity of DMF with the "naked eye" at a sensitivity far beyond the "naked nose". We conclude that the panchromatic hypersensitivity toward the environment of the new cNDIs is ideal for pattern generation in differential sensing arrays.

Introduction

Core-substituted naphthalenediimides (cNDIs) are 1,4,5,8-napththalenediimides (NDIs, **1**) with one or more substituents in position 2, 3, 6 or 7 (Fig. 1).[1–12] With electron donors in the core, cNDIs become panchromatic push–pull fluorophores, electron acceptors yield the strongest π-acids known today.[1] cNDIs are wonderful fluorophores, covering all primary colors by exchange of single atoms only.[1–8] Formal substitution of one oxygen atom in the core of the yellow fluorophore **2** by a nitrogen yields red fluorophore **3**. Substitution of the other oxygen with another nitrogen is sufficient to cover the primary colors.[2,3] Formal addition of two more alkylamino groups converts the blue cNDI **4** into the green chlorophyll mimic **5**.[4] Decreasing LUMO energies with increasing bandgap identifies cNDIs as ideal for the construction of multicomponent photosystems with operational redox gradients that do not suffer from low-energy traps.[5]

cNDIs with electron acceptors in the core are attractive because their exceptional π-acidity provides access to one of the few air-stable n-semiconductors as well as to powerful anion transporters.[8–12] The most π-acidic cNDI **6** has an inverted quadrupole moment of an unprecedented +39 Buckinghams.[11] The synthesis of tetracyano cNDIs failed despite significant efforts.[11] To increase the π-acidity, we recently applied redox chemistry.[12] The "super-π-acid" **7** was readily synthesized by oxidation of the four sulfides in the core of cNDI **8**. Successful at one extreme of the cNDI series, we speculated that either acid–base or redox chemistry could be used to break records at the other extreme as well, that is with electron-rich cNDIs. In many panchromatic systems, including green to red fluorescent proteins,[13] phenolate anions serve as the ultimate π-donors. Deprotonation of cNDIs such as **9** with a hydroquinone core should thus easily provide access to absorption maxima beyond the 642 nm of tetraamino cNDI **5**. (With core expanded cNDI, bathochromic shifts up to 692 nm have been reported, for cNDI polymers with conjugated cores, the NIR frontier is at 985 nm.)[8] In the following, we report that this expectation turned out to be incorrect, also for the similarly panchromatic, pH-responsive cNDIs **10** with catechols in the core, and for their boronic esters. However, the expanded core-substituted perylenediimide (cPDI)[14] **11** shifted to 760 nm upon deprotonation with base, 74 nm (1419 cm^{-1}) beyond the previously reported diamino cPDI. As an alternative approach to the NIR frontier with the most compact cNDI fluorophores, lessons from sea anemone and corals on how to make the green-fluorescent protein from the jellyfish fluoresce in red[13] were applied, that is oxidative imination, the same strategy that accounts for the chemistry of vision.[15]

School of Chemistry and Biochemistry, University of Geneva, Geneva, Switzerland. E-mail: stefan.matile@unige.ch; Fax: +41 22 379 5123; Tel: +41 22 379 6523; Web: www.unige.ch/sciences/chiorg/matile

† In memory of Philippe Perrottet.

‡ Electronic supplementary information (ESI) available: Detailed experimental procedures. See DOI: 10.1039/c1ob05702b

§ These two authors contributed equally to this work.

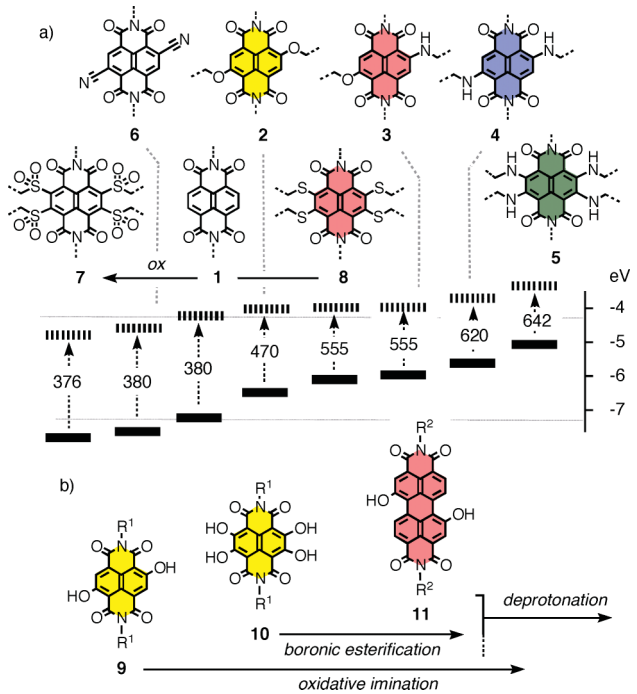

Fig. 1 (a) Previously reported cNDIs with HOMO/LUMO levels and absorption maxima in nm, with super-π-acid **8** obtained with redox chemistry from **7**. (b) Panchromatic cNDIs reported in this study to maximize bathochromism with acid–base chemistry, boronic esterification and oxidative imination (R^1 = mesityl, R^2 = cyclohexyl).

Results and discussion

The synthesis of cNDI **9** with a hydroquinone core was very straightforward (Scheme 1). Dibromo cNDI **12** was prepared from naphthalene dianhydride following recent procedures from the literature.[16] Nucleophilic substitution in the core with allyl alcohol gave the yellow cNDI **13** in excellent yield. Pd-catalyzed deallylation afforded the hydroquinone in the core of **9** selectively and under mild conditions. The cNDI **10** with catechols in the core and the expanded cPDI **11** were prepared analogously. Detailed procedures and analytical data for all new compounds are given in the ESI.‡[17]

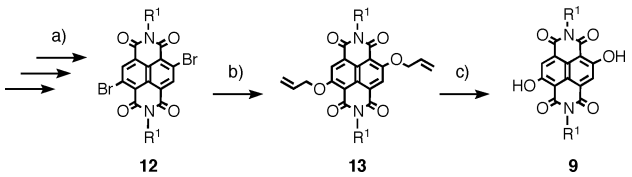

Scheme 1 Synthesis of cNDI **9** with a hydroquinone core. a) Naphthalene dianhydride, several reported steps.[16] b) Allyl alcohol, NaH, dichloromethane, 4 Å MS, 4 h, rt, 86%. c) $Pd(PPh_3)_4$, phenylsilane, dichloromethane, 4 Å MS, 10 h, rt, 80% (R^1 = mesityl).

The absorption spectrum of cNDI **9** in a 4 : 1 mixture of DMSO and water at pH 3 showed a maximum at 470 nm (Fig. 2 and 3, Table 1). With increasing pH, this maximum exhibited a spectacular, biphasic bathochromic shift. The first shift occurred at an apparent $pK_a = 6.3$ (Fig. 4●, Table 1). The strong acidity of the first hydroxy group originated presumably from the stabilization of the conjugate base **14** by resonance with the withdrawing imides. The second shift occurred at $pK_a = 11.1$ (Fig. 4●, Table 1). The weak acidity of the second hydroxy group appeared reasonable considering intramolecular charge repulsion[18] in dianion **15**. The absorption maximum of the conjugate base **15** was found at 615 nm. This places the maximum of cNDI **15** 27 nm (684 cm^{-1}) below that of the tetramino cNDI **5** at 642 nm (Fig. 1–3, Table 1).

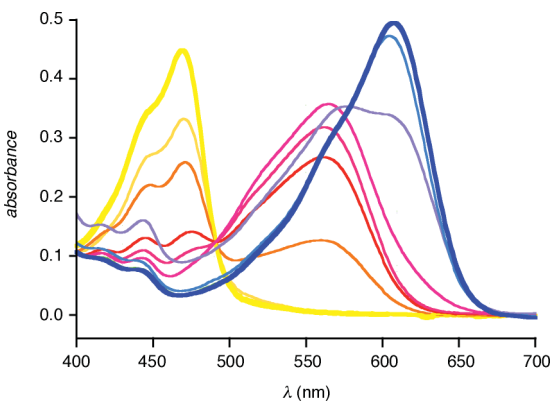

Fig. 2 Changes in the absorption spectra of **9** with increasing pH from pH 3 (yellow) to pH 12 (blue) in DMSO/water 4 : 1, 25 °C.

Table 1 Spectroscopic properties of cNDIs and cPDIs

Entry	cNDIs	λ_{abs} (nm)[a]	ε (M^{-1} cm^{-1})[b]	λ_{em} (nm)[c]	τ (ns)[d]	Φ_{fl} (%)[e]	pK_a[f]
1	**9**	470	12 000	500, 630[g]	<0.1, 1.1[g]	1	6.3 (7.2)
2	**14**	565[h]	10 200[h]				11.1 (11.5)
3	**15**	615	15 200	661	12.7	64	
4	**10**	490	4200	520, 610[g]	0.8, 1.9[g]	6	3.7
5	**17**	513[i]	4000[i]				9.3
6	**18**	570[i]	3900[i]				12.8
7	**19**	640[i]	6900[i]				
8	**11**	570	6600	600	1.1	6	7.3 (8.0)
9	**20**	708[h]	11 500[h]				10.4 (10.6)
10	**21**	760	20 400	820	0.9	2	

[a] Absorption maximum at longest wavelength, in nanometres, measured in DMSO/water 4 : 1, 25 °C, at appropriate pH. pH values were measured in DMSO/water 4 : 1 and used without correction. A 10 mM triethanolamine buffer was present if appropriate. The absorption maxima can be highly sensitive to changes in environment, the reported values are thus subject to minor variations, particularly with intermediate conjugate bases. [b] Extinction coefficient. [c] Emission maxima, if applicable. Spectra with unresolved excitation maxima are not reported. [d] Fluorescence lifetime. [e] Fluorescence quantum yield in percent. [f] pK_a in DMSO/water 4 : 1, 25 °C, from Hill analysis of pH profiles. Values in parenthesis are from HypSpec analysis. [g] Two emission maxima, see Fig. 3, 5, and text. [h] Computed approximations from HypSpec analysis. [i] Apparent value without further analysis.

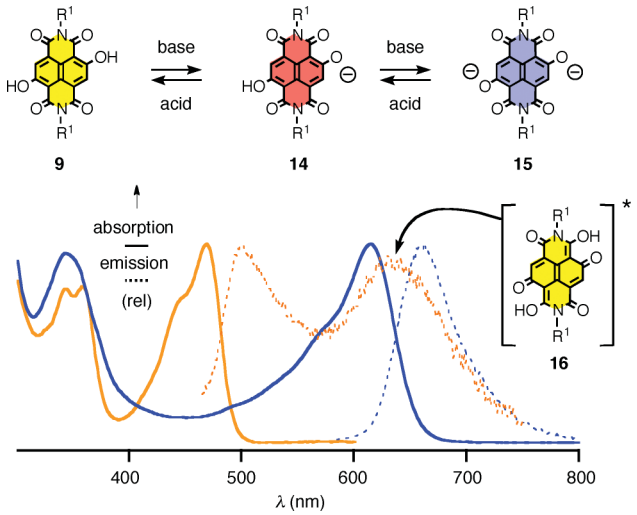

Fig. 3 Absorption (solid) and emission spectra (dotted) of **9** (pH 3, yellow) and **15** (pH 13, blue) in DMSO/water 4 : 1, 25 °C, normalized to 1 at their maxima.

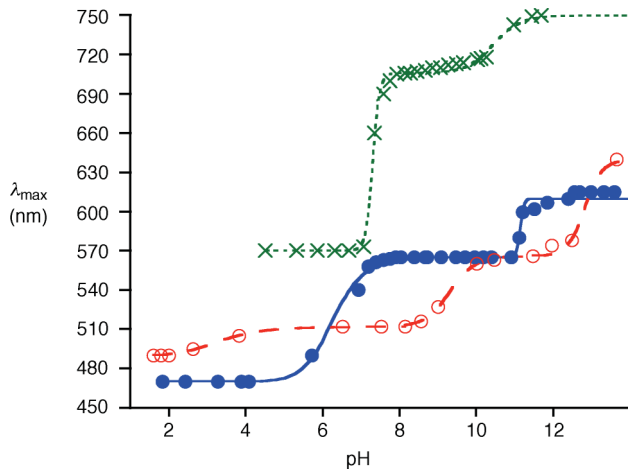

Fig. 4 Absorption maxima of **9** (●), **10** (○) and **11** (×) as a function of pH.

Similar to the alkoxy cNDIs **2**,[1] hydroquinone cNDI **9** showed green fluorescence (Fig. 3, Table 1). However, the fluorescence quantum yield was with $\Phi_{fl} = 1\%$ very poor, much poorer than the $\Phi_{fl} = 22\%$ reported for dialkoxy cNDIs. The very short lifetime $\tau < 100$ ps of the excited state was in agreement with the poor quantum yield of the high energy emission.

A second, equally strong emission maxima was observed at 630 nm (Fig. 3, Table 1). This bathochromic emission maximum appeared only in water-containing solvent mixtures. The excited state accounting for the low-energy emission was populated from the one accounting for the high-energy emission at 500 nm and decayed with a clearly longer $\tau = 1.1$ ns (Table 1). These observations supported the occurrence of excited-state intramolecular proton transfer (ESIPT)[19] and red-shifted emission from the excited-state tautomer **16**. Consistent with this interpretation, ESIPT emission was even stronger with the cNDI **10** with four hydrogen-bond donors in the core but absent with cPDI **11** without hydrogen-bond acceptor in the core (see below and Table 1). Similar observations have been reported previously with a different explanation for core-expanded NDIs.[7b] More detailed studies on the ultrafast photophysics of this ESIPT emission are ongoing and will be reported in due course.

Unambiguous assignment of the absorption and emission maxima of the singly deprotonated intermediate **14** was problematic because of overlapping and shifting signals (Fig. 2). Deconvolution of the overlapping spectra of the individual chromophores by HypSpec analysis[20] located the absorption maximum at 565 nm (Fig. S3, ESI,‡ Table 1, entry 2). The same analysis gave a pK_a = 7.2. This result suggested that the effective acidity of hydroquinone **9** is poorer than expected from the apparent $pK_a = 6.3$ obtained from the pH profile (Fig. 4, Table 1). The emission maximum is not reported because it was not possible to identify a single species in the excitation spectra.

Dianion **15** emitted at 661 nm (Fig. 3, Table 1). The fluorescence quantum yield increased significantly from $\Phi_{fl} = 1\%$ for protonated cNDI to $\Phi_{fl} = 64\%$ for deprotonated dianion **15** (Table 1). This increase was correctly reflected by a decelerated fluorescence decay from $\tau < 100$ ps for protonated **9** to $\tau = 12.7$ ns for deprotonated **15** (Table 1). These consistent trends suggested that ESIPT accounts for the poor fluorescence of cNDIs with hydrogen bond donors in the core.

In neutral form at pH ~ 2, cNDI **10** with catechols in the core absorbed at 490 nm, that is 20 nm (869 cm^{-1}) red shifted from cNDI **9** with only two π-donors in the core (Fig. 5). This is unlike the tetraalkoxy-NDI, which exhibited 50 nm (2544 cm^{-1}) blue shift compared to di-alkoxy-NDI.[4] The emission at 520 nm was complemented by a second maximum at 610 nm. The increased intensity of this bathochromic emission with four hydrogen-bond donors in the core of cNDI **10** compared to two donors in **9** was consistent with ESIPT.

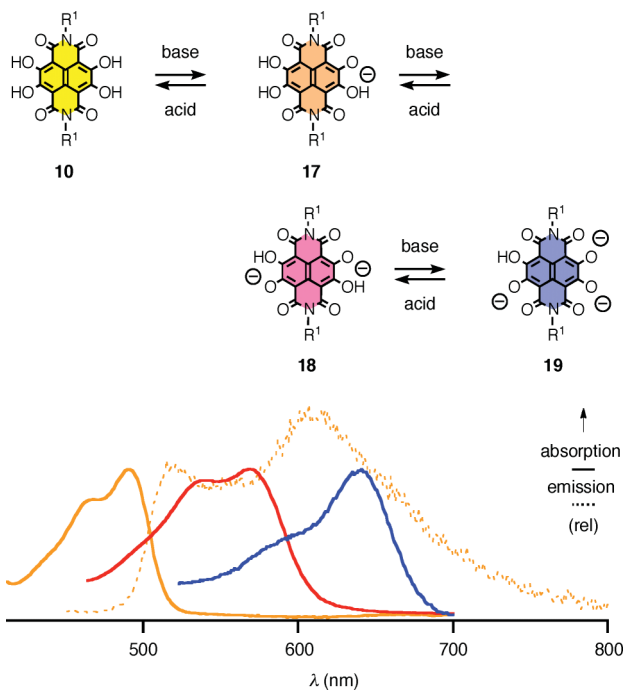

Fig. 5 Absorption (solid) and emission spectra (dotted) of **10** (pH 2, yellow) and absorption spectra of **18** (pH 9, red) and **19** (pH 14, blue) in DMSO/water 4 : 1, 25 °C. High-energy regions for **18** and **19** were removed because they were contaminated by oxidative degradation products.

With cNDI **10**, the interpretation of the spectroscopic changes in response to increasing pH became even more complex than with cNDI **9** (Fig. S1). A small gradual shift at low pH suggested that removal of the first proton occurs already at pK_a = 3.7 (Fig. 4○). The apparent maximum of the monoanion **17**, could however not be clearly identified. The high acidity of catechol **10** was reasonable considering stabilization of the conjugated base **17** by hydrogen bonding and resonance, and because of probability effects related to multivalency.[18] Moreover, the next clear shift to 570 nm occurred at pK_a = 9.3, an acidity that appeared too weak to originate from catechol **10** (Fig. 4○).

Intramolecular hydrogen bonding probably also accounts for the reduced bathochromic shift to 570 nm of the conjugate base **18**, that is 45 nm (1284 cm^{-1}) less than the corresponding dianion **15** (Table 1). Further deprotonation of the putative dianion **18** was just detectable at pK_a = 12.8. The absorption maximum of the putative trianion **19** was at 640 nm, that is at the current NIR frontier marked by tetraamino cNDIs **5** (Fig. 5 and 1, Table 1). Further deprotonation was not observable, also, with NaH in aprotic solvents, competing oxidative degradation made processes under basic conditions difficult to follow. Emission spectra of deprotonated catechol cNDIs **17–19** could not be attributed to single compounds and are thus not reported.

Charge-free at pH ~ 2, the disubstituted cPDI **11** with a hydroquinone core absorbed at 570 nm (Fig. 6). This is 100 nm (3733 cm^{-1}) bathochromic from the disubstituted cNDI **9** at 470 nm (Table 1). This red-shift originated from the expanded aromatic system in the perylene core, PDIs without substituents in the core already absorb at 526 nm.[14] cPDI **11** emitted at 600 nm without second emission maximum at low energy (Fig. 6). The disappearance of the second emission maximum with increasing distance between hydrogen-bond donors in the core and imide acceptors in cPDI **11** was in agreement with ESIPT as origin of the bathochromic emission with cNDIs **9** and **10**. ESIPT could thus not account for the rather low Φ_{fl} = 6% and the relatively short τ = 1.1 ns of cPDI **11** (Table 1).[21]

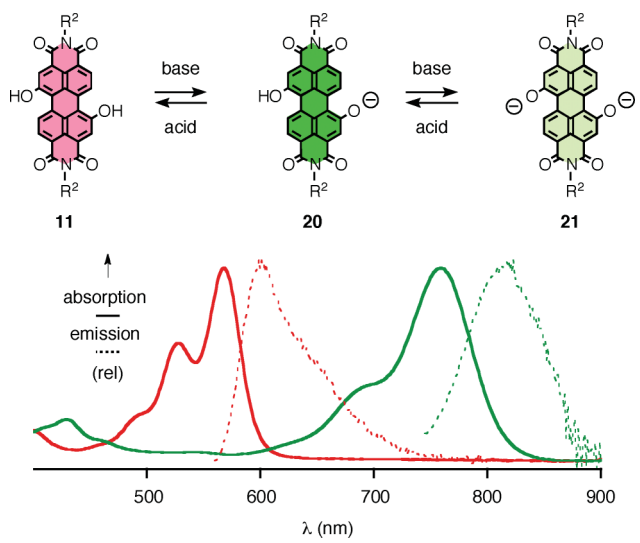

Fig. 6 Absorption (solid) and emission spectra (dotted) of **11** (pH 5, red) and **21** (pH 12, green) in DMSO/water 4 : 1, 25 °C (R^2 = cyclohexyl).

Removal of the first proton occurred at pK_a = 7.3 (Fig. 4× and S2, ESI‡). This comparably poor acidity suggested that the stabilization of the conjugate base **20** by resonance with the withdrawing imides is less powerful than with cNDIs, perhaps due to the deplanarization of the PDI core. HypSpec analysis of all overlapping bands further reduced the acidity to pK_a = 8.0 and placed the absorption of the cPDI monoanion **20** at 708 nm (Fig. S4, ESI,‡and Table 1). This calculated to a red shift of 138 nm (3420 cm^{-1}) for the first deprotonation for cPDI **11** compared to 95 nm (3578 cm^{-1}) for the homologous cNDI **9**.

The deprotonation of monoanionic cPDI **20** occurred at pK_a = 10.4 (Fig. 4×). The resulting cPDI dianion **21** absorbed at 760 nm and emitted at 820 nm. Contrary to the situation with cNDI **15**, the removal of hydrogen-bond donors in the core did not improve the poor fluorescence quantum yield Φ_{fl} = 2% of the emission of cPDI **21** at 820 nm. Insensitivity was not surprising because intramolecular hydrogen bonding including ESIPT does not account for the poor fluorescence of hydroquinone cPDI **11**.

The red shift of 52 nm (966 cm^{-1}) for the second cPDI deprotonation was in the range of the corresponding cNDIs. Whereas dianionic cNDIs **15** and **18** failed to exceed the absorption of diamino cNDIs **4**, dianionic cPDIs **21** absorbed 74 nm (1419 cm^{-1}) beyond diamino cPDIs. Barely visible with the "naked eye", their NIR absorption is unprecedented in the cPDI series.[14]

The absorption maxima of cNDIs and cPDIs **9–11** did not show a linear dependence on the polarity of the solvent (Fig. 7a). This was meaningful because their pull–push–pull architecture results in a globally symmetric molecule, where solvent stabilization by dipole–dipole interactions is not possible. However, the absorption maxima of cNDIs and cPDIs **9–11** showed a roughly linear dependence on the Lewis basicity[22] of the solvent (Fig. 7b). Minor deviations are readily explicable with the quality and age of the solvent (Fig. 8).

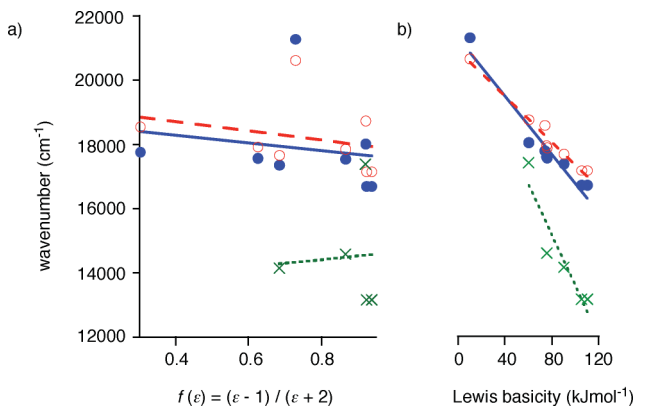

Fig. 7 Absorption maxima of **9** (●), **10** (○) and **11** (×) in wavenumbers as a function of (a) the polarity function f(ε) and (b) $-\Delta H_0^{BF3}$ (295.15), the Lewis basicity of the solvent.

The large shifts obtained for small differences in the Lewis basicity of the environment were intriguing and called for practical applications. For instance, commercial and freshly distilled DMF could be distinguished with the naked eye after adding a drop of cNDI **9** (Fig. 8a). Ratiometric detectability of the purity of DMF was ideal for quantitative analysis. The ratio of the red absorption at 538 nm and the blue absorption at 610 nm of cNDI in DMF purchased from commercial suppliers was

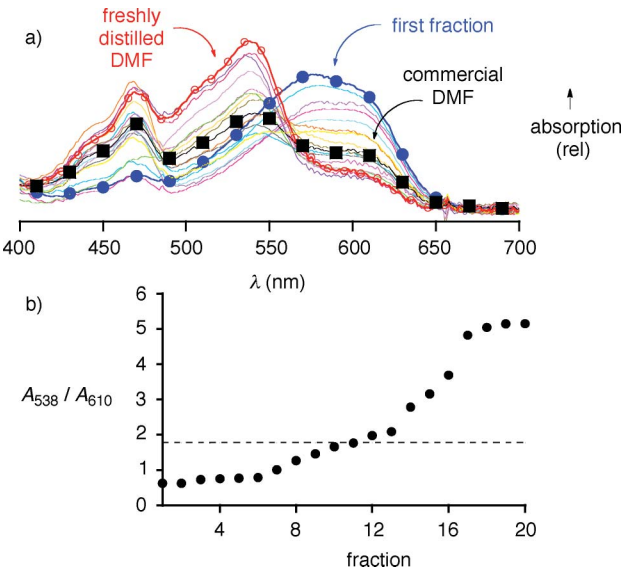

Fig. 8 a) Absorption spectra of cNDI **9** added to the early fractions (2 ml each; fraction 1, ●; fraction 20, ○) of the distillation of commercial DMF (■). b) Fractional absorption A_{538}/A_{610} of **9** in the early fractions of DMF distillation (●) compared to commercial DMF (dashed).

at A_{538}/A_{610} = 1.77 (Fig. 8a■; 8b, dashed line). Distillation of commercial DMF produced first fractions of A_{538}/A_{610} < 1.0 (Fig. 8a●, 8b●). This high basicity of the first fractions of distilled DMF properly reflects the enrichment with the low-boiling dimethylamine impurities. Ultrapure DMF obtained in the later fractions saturated A_{538}/A_{610} = 5.15 (Fig. 8a○, 8b●). DMF with $A_{538}/A_{610} \geq 3.0$ was odorless. Remarkably, cNDI **9** thus visualizes the purity of DMF for the "naked eye" with a sensitivity that is far beyond the sensitivity of the "naked nose".

The conversion of catechols in the core of cNDI **10** into boronic esters in cNDI **22** was explored with phenylboronic acid (PBA, Fig. 9● and Fig. 10).[23–26] The absorption at pH = 8.0 showed a weak red shift with increasing PBA concentration. Hill analysis of the dose response curve gave an apparent dissociation constant K_D = 3.7 ± 0.1 mM. This value was in the range observed for

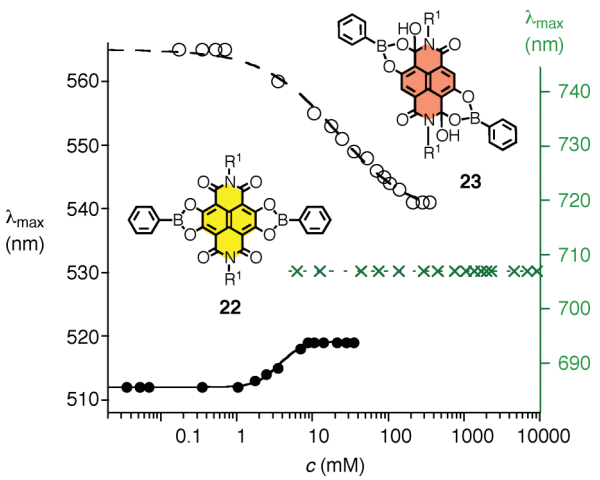

Fig. 9 Absorption maxima of **9** (○), **10** (●) and **11** (×) in DMSO/water 4 : 1 at pH 8.0 as a function of the concentration of phenylboronic acid (PBA).

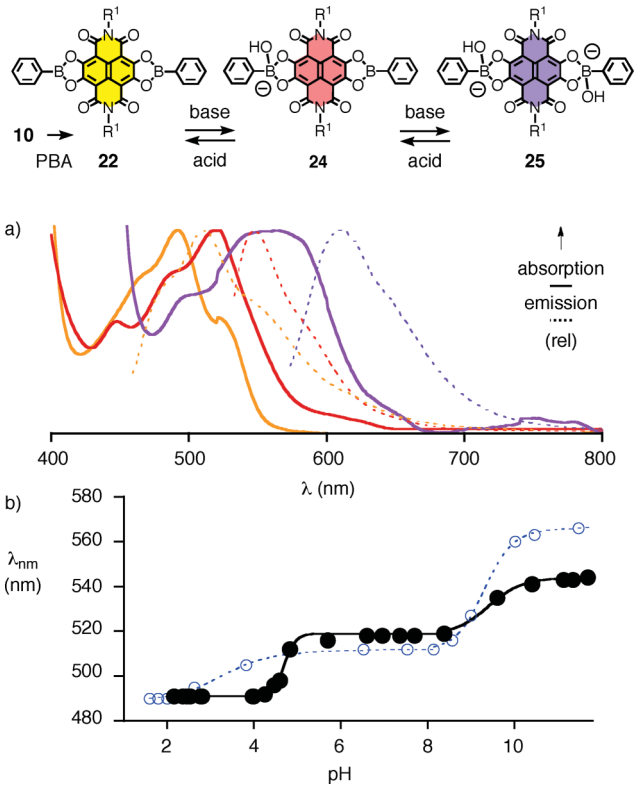

Fig. 10 a) Absorption (solid) and emission (dotted) spectra of **22** (pH 3, orange), **24** (pH 7, red) and **25** (pH 11, violet) in DMSO/water 4 : 1, 25 °C. b) Absorption maxima of **22** (●) and **10** (○) as a function of pH.

other catechols under similar conditions.[23–26] The insensitivity of the absorption maximum to up to 10 M PBA was in agreement with the inability of cPDI **11** to form boronic esters, (Fig. 9×). cNDI **9** showed a relatively large hypsochromic shift of 24 nm (1145 cm^{-1}) at K_D = 21.8 ± 2.3 mM in response to PBA (Fig. 9○). Intramolecular reaction of the boronic acid semi-ester with the proximal imide carbonyl group would be consistent with this behavior.[23–26] Dehydroxylation of the obtained chromophore **23** is further conceivable (Fig. 9).

In neutral form at pH < 3, the absorption of cNDI **22** at 486 nm was poorly distinguishable from the one at 490 nm of the free catechol **10** (Fig. 10). However, deprotonation of the first hydrated boronic ester occurred with a sharp, distinctive red shift at pK_a = 4.7 (Fig. 10b●). This acidity of the boronic ester was as expected from the literature.[23–26] It was consistent with the lack of resonance with the NDI core and an only weak influence from the imide acceptors.

Deprotonation of the hydrated conjugate base **24** was with pK_a = 9.4 more difficult because of intramolecular charge repulsion.[18] The final absorption of the boronate ester dianion **25** at 544 nm was 26 nm (838 cm^{-1}) less red-shifted than that of the putative catechol dianion **18**. Poor sensitivity of boronic ester **22** to increasing pH was consistent with the lack of resonance with the cNDI core. At pH > 12, the absorption increased rapidly due to partial hydrolysis of the boronate esters in cNDI **25**.

cNDIs **22**, **24** and **25** with boronic acid esters in the core were fluorescent (Fig. 10a). Absorptions and emissions measured for cNDI boronate esters were often broad and had unusual shapes. Although contributions from decreasing extinction coefficients

deserve consideration (**25**: $\varepsilon = 1.8\ mM^{-1}\ cm^{-1}$), these unsatisfactory spectra indicated the presence of several absorbing and emitting species under all conditions. This more complex situation with cNDIs with boronate esters in the core was not further investigated because it deviated from the topic of the study.

The oxidation of hydroquinone **9** with ceric ammonium nitrate (CAN) followed by covalent capture of the intermediate naphthoquinone with arylamines gave green cNDIs **26–31** with an iminoquinone, their protonation gave the iminium cNDI **32–37** (Fig. 11). Aniline gave the green cNDI **26** with an iminoquinone core (Fig. 11a). With aniline, the absorption maximum shifted to 638 nm, that is 4 nm (98 cm^{-1}) below that of tetraamino cNDI **5**. Protonation of the first imine of iminoquinone **26** at $pK_a = 5.8$ caused a significant hypsochromic shift (2088 cm^{-1}) to 563 nm (Fig. 11). The blue-shifted, very broad absorption of iminium cNDI **32** was consistent with the at least partial conversion of the π-donating imine into a strong π-acceptor (Fig. 11a). Additional π-donors in the *para*-position had little influence in the spectroscopic properties of imino cNDIs **27** and **28** and their conjugate acids **33** and **34** (Fig. 11b). Poor sensitivity to substituent effects confirmed that, for steric reasons, the aryl groups are poorly conjugated with the iminoquinone core. Nitro acceptors in the *meta*-position of imino cNDI **29** shifted the absorption to 627 nm without changing the pK_a much. This small blue-shift was consistent with the weakening of the imine π-donor by the nitro acceptor. Hydroxy donors in the *ortho*-position of **30** shifted the absorption of the iminium cNDI **36** to 528 nm. Competing intramolecular hydrogen bonding to the hydroxy lone pairs is likely to account for this more important bathochromic effect. The simultaneous decrease in acidity to $pK_a = 6.8$ reflects the hybrid between a poorly acidic phenol and a highly acidic aryl iminium proton. Iminium cNDI **37** with *ortho*-methoxy instead of hydroxy groups naturally lost the reduced acidity but preserved the bathochromic shift of cNDI **36**.

Conclusions

Synthesis and characterization of naphthalene- and perylenediimides with hydroquinones, catechols, boronic esters and iminoquinones in the core are described. They enrich the current collection of cNDI and cPDI in a colorful manner. As in green and red fluorescent proteins from jellyfish and corals, phenoxy and imine groups are identified as powerful π-donors to approach the NIR frontier. The dynamic covalent chemistry realized with catechols and boronic acids on the one hand and quinones and amines on the other hand provides an attractive tool to modulate optoelectronic properties *in situ* and to quickly build multicomponent architectures, *e.g.* layer-by-layer assembly on solid surfaces.[27] Particularly impressive is the ability of hydroquinone cNDIs to cover all primary colors by simple changes in pH. This panchromatic responsiveness to the environment is of practical use to sense the purity of DMF with the "naked eye" at sensitivities far beyond the "naked nose". This example of panchromatic hypersensitivity demonstrates that the new cNDIs will be ideal for pattern generation in differential sensing arrays.[28]

Acknowledgements

We thank A. Vargas Jentzsch, J. Areephong and T. M. Fyles (University of Victoria, Canada) for contributions to data

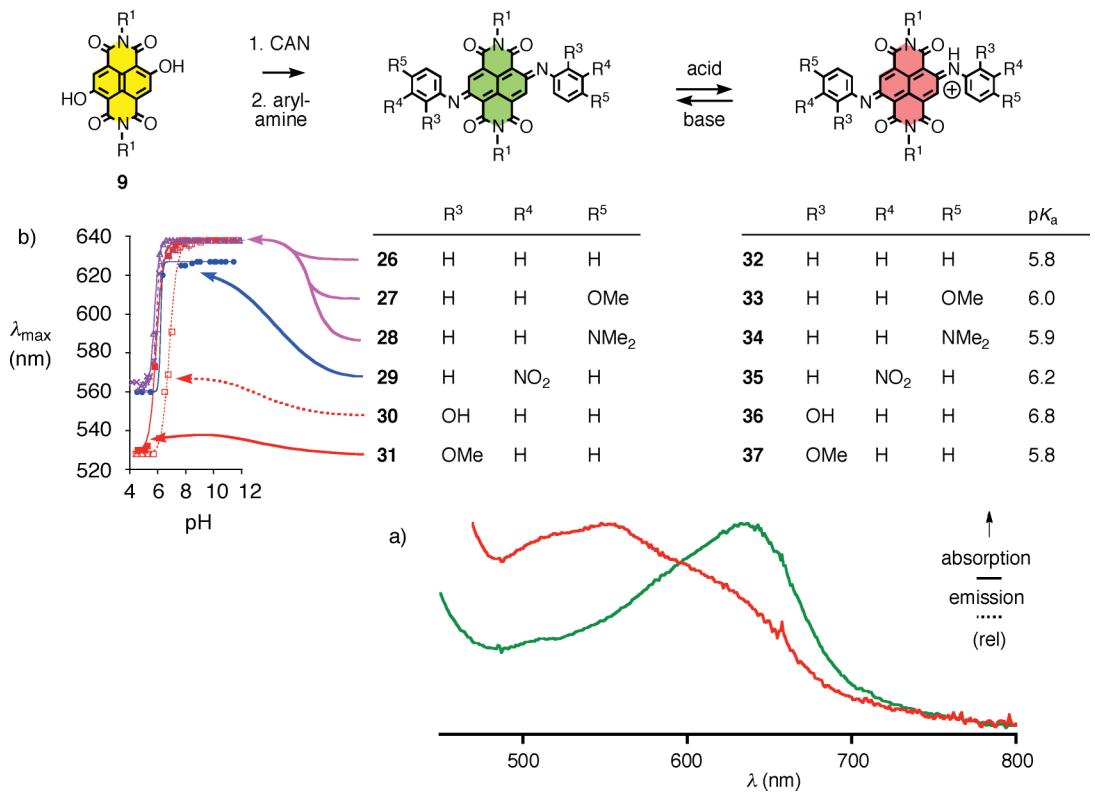

	R³	R⁴	R⁵		R³	R⁴	R⁵	pKa
26	H	H	H	**32**	H	H	H	5.8
27	H	H	OMe	**33**	H	H	OMe	6.0
28	H	H	NMe_2	**34**	H	H	NMe_2	5.9
29	H	NO_2	H	**35**	H	NO_2	H	6.2
30	OH	H	H	**36**	OH	H	H	6.8
31	OMe	H	H	**37**	OMe	H	H	5.8

Fig. 11 a) Absorption spectra of **26** (pH 9, green) and **32** (pH 4, red) in DMSO/water 4 : 1, 25 °C. b) Change in absorption maxima of imines **26–31** upon protonation with decreasing pH to give iminium cations **32–37**.

collection and analysis, N.-T. Lin and D.-H. Tran for contributions to synthesis, D. Jeannerat, A. Pinto and S. Grass for NMR measurements, the Sciences Mass Spectrometry (SMS) platform for mass spectrometry services, and the University of Geneva, the European Research Council (ERC Advanced Investigator, S.M.), the National Centre of Competence in Research (NCCR) Chemical Biology (S.M.), the NCCR MUST (E.V.) and the Swiss NSF (S.M., E.V.) for financial support.

Notes and references

1 N. Sakai, J. Mareda, E. Vauthey and S. Matile, *Chem. Commun.*, 2010, **46**, 4225–4237.

2 F. Würthner, S. Ahmed, C. Thalacker and T. Debaerdemaeker, *Chem.–Eur. J.*, 2002, **8**, 4742–4750.

3 R. S. K. Kishore, O. Kel, N. Banerji, D. Emery, G. Bollot, J. Mareda, A. Gomez-Casado, P. Jonkheijm, J. Huskens, P. Maroni, M. Borkovec, E. Vauthey, N. Sakai and S. Matile, *J. Am. Chem. Soc.*, 2009, **131**, 11106–11116.

4 C. Röger and F. Würthner, *J. Org. Chem.*, 2007, **72**, 8070–8075.

5 (*a*) N. Sakai, R. Bhosale, D. Emery, J. Mareda and S. Matile, *J. Am. Chem. Soc.*, 2010, **132**, 6923–6925; (*b*) R. Bhosale, A. Perez-Velasco, V. Ravikumar, R. S. K. Kishore, O. Kel, A. Gomez-Casado, P. Jonkheijm, J. Huskens, P. Maroni, M. Borkovec, T. Sawada, E. Vauthey, N. Sakai and S. Matile, *Angew. Chem., Int. Ed.*, 2009, **48**, 6461–6464; (*c*) A. L. Sisson, N. Sakai, N. Banerji, A. Fürstenberg, E. Vauthey and S. Matile, *Angew. Chem., Int. Ed.*, 2008, **47**, 3727–3729; (*d*) N. Sakai, A. L. Sisson, T. Bürgi and S. Matile, *J. Am. Chem. Soc.*, 2007, **129**, 15758–15759; (*e*) S. Bhosale, A. L. Sisson, P. Talukdar, A. Fürstenberg, N. Banerji, E. Vauthey, G. Bollot, J. Mareda, C. Röger, F. Würthner, N. Sakai and S. Matile, *Science*, 2006, **313**, 84–86.

6 (*a*) S. Gabutti, S. Schaffner, M. Neuburger, M. Fischer, G. Schäfer and M. Mayor, *Org. Biomol. Chem.*, 2009, **7**, 3222–3229; (*b*) C. W. Marquardt, S. Grunder, A. Błaszczyk, S. Dehm, F. Hennrich, H. V. Löhneysen, M. Mayor and R. Krupke, *Nat. Nanotechnol.*, 2010, **5**, 863–867.

7 (*a*) S. Bhosale, M. Kalyankar, S. Bhosale, S. J. Langford, E. Reid and C. Hogan, *New J. Chem.*, 2009, **33**, 2409–2413; (*b*) H. Langhals and S. Kinzel, *J. Org. Chem.*, 2010, **75**, 7781–7784; (*c*) S. M. Hampel, A. Sidibe, M. Gunaratnam, J.-F. Riou and S. Neidle, *Bioorg. Med. Chem. Lett.*, 2010, **20**, 6459–6463; (*d*) W. Yue, Y. Zhen, Y. Li, W. Jiang, A. Lv and Z. Wang, *Org. Lett.*, 2010, **12**, 3460–3463; (*e*) X. Lu, W. Zhu, Y. Xie, X. Li, Y. Gao, F. Li and H. Tian, *Chem.–Eur. J.*, 2010, **16**, 8355–8364.

8 (*a*) S. Chopin, F. Chaignon, E. Blart and F. Odobel, *J. Mater. Chem.*, 2007, **17**, 4139–4146; (*b*) H. Krüger, S. Janietz, D. Sainova, D. Dobreva, N. Koch and A. Vollmer, *Adv. Funct. Mater.*, 2007, **17**, 3715–3723; (*c*) X. Guo and M. D. Watson, *Org. Lett.*, 2008, **10**, 5333–5336.

9 B. A. Jones, A. Facchetti, M. R. Wasielewski and T. J. Marks, *J. Am. Chem. Soc.*, 2007, **129**, 15259–15278.

10 (*a*) J.-H. Oh, S.-L. Suraru, W.-Y. Lee, M. Könemann, W. Höffken, C. Röger, R. Schmidt, Y. Chung, W.-C. Chen, F. Würthner and Z. Bao, *Adv. Funct. Mater.*, 2010, **20**, 2148–2156; (*b*) X. Gao, C. Di, Y. Hu, X. Yang, H. Fan, F. Zhang, Y. Liu, H. Li and D. Zhu, *J. Am. Chem. Soc.*, 2010, **132**, 3697–3699.

11 R. E. Dawson, A. Hennig, D. P. Weimann, D. Emery, S. Gabutti, J. Montenegro, V. Ravikumar, M. Mayor, J. Mareda, C. A. Schalley and S. Matile, *Nat. Chem.*, 2010, **2**, 533–538.

12 J. Misek, A. Vargas Jentzsch, S. Sakurai, D. Emery, J. Mareda and S. Matile, *Angew. Chem., Int. Ed.*, 2010, **49**, 7680–7683.

13 R. Y. Tsien, *Angew. Chem., Int. Ed.*, 2009, **48**, 5612–5626.

14 (*a*) F. Würthner, *Chem. Commun.*, 2004, 1564–1579; (*b*) Y. Zhao and M. R. Wasielewski, *Tetrahedron Lett.*, 1999, **40**, 7047–7050.

15 B. Borhan, M. L. Souto, H. Imai, Y. Shichida and K. Nakanishi, *Science*, 2000, **288**, 2209–2212.

16 R. S. K. Kishore, V. Ravikumar, G. Bernardinelli, N. Sakai and S. Matile, *J. Org. Chem.*, 2008, **73**, 738–740.

17 See ESI‡.

18 B. Baumeister, A. Som, G. Das, N. Sakai, F. Vilbois, D. Gerard, S. P. Shahi and S. Matile, *Helv. Chim. Acta*, 2002, **85**, 2740–2753.

19 (*a*) J. Wu, W. Liu, J. Ge, H. Zhang and P. Wang, *Chem. Soc. Rev.*, 2011, **40**, 3483–3495; (*b*) M. Y. Berezin and S. Achilefu, *Chem. Rev.*, 2010, **110**, 2641–2684; (*c*) A. S. Klymchenko and A. P. Demchenko, *Methods Enzymol.*, 2008, **450**, 37–58.

20 (*a*) A. Braibanti, G. Ostacoli, P. Paoletti, L. D. Pettit and S. Sammartano, *Pure Appl. Chem.*, 1987, **59**, 1721–1728; (*b*) P. Gans, A. Sabatini and A. Vacca, *Talanta*, 1996, **43**, 1739–1753.

21 In a publication appearing just before submission of this manuscript, a blue shift to 512 nm was reported for cPDIs with four OH groups in positions 2, 5, 8 and 11, that is next to the imide carbonyls and not in the more reactive bay region. This counterintuitive hypsochromic effect was explained by intramolecular hydrogen bonding to the imide carbonyls. ESIPT was absent in all emission spectra because they were not recorded in water-containing media: T. Teraoka, S. Hiroto and H. Shinokubo, *Org. Lett.*, 2011, **13**, 2532–2535.

22 P.-C. Maria and J.-F. Gal, *J. Phys. Chem.*, 1985, **89**, 1296–1304.

23 T. D. James, *Top. Curr. Chem.*, 2007, **277**, 107–152.

24 (*a*) C. M. Bromba, P. Carrie, J. K. W. Chui and T. M. Fyles, *Supramol. Chem.*, 2009, **21**, 81–88; (*b*) G. Springsteen and B. Wang, *Tetrahedron*, 2002, **58**, 5291–5300.

25 A. Hennig, S. Hagihara and S. Matile, *Chirality*, 2009, **21**, 826–835.

26 (*a*) N. Y. Edwards, T. W. Sager, J. T. McDevitt and E. V. Anslyn, *J. Am. Chem. Soc.*, 2007, **129**, 13575–13583; (*b*) N. Lin, J. Yan, Z. Huang, C. Altier, M. Li, N. Carrasco, M. Suyemoto, L. Johnston, S. Wang, Q. Wang, H. Fang, J. Caton-Williams and B. Wang, *J. Am. Chem. Soc.*, 2008, **130**, 12636–12638; (*c*) T. D. James, K. R. A. S. Sandanayake and S. Shinkai, *Nature*, 1995, **374**, 345–347; (*d*) J. Yoon and A. W. Czarnik, *Bioorg. Med. Chem.*, 1993, **1**, 267–271; (*e*) S. Hagihara, H. Tanaka and S. Matile, *J. Am. Chem. Soc.*, 2008, **130**, 5656–5657.

27 (*a*) R. Bhosale, J. Misek, N. Sakai and S. Matile, *Chem. Soc. Rev.*, 2010, **39**, 138–149; (*b*) N. Sakai, A. L. Sisson, T. Bürgi and S. Matile, *J. Am. Chem. Soc.*, 2007, **129**, 15758–15759; (*c*) A. L. Sisson, N. Sakai, N. Banerji, A. Fürstenberg, E. Vauthey and S. Matile, *Angew. Chem., Int. Ed.*, 2008, **47**, 3727–3729; (*d*) G. Decher, *Science*, 1997, **277**, 1232–1237; (*e*) H. M. El-Kaderi, J. R. Hunt, J. L. Mendoza-Cortés, A. P. Côté, R. E. Taylor, M. O'Keeffe and O. M. Yaghi, *Science*, 2007, **316**, 268–272; (*f*) A. I. Cooper, *Angew. Chem., Int. Ed.*, 2011, **50**, 996–998; (*g*) K. Severin, *Dalton Trans.*, 2009, 5254–5264; (*h*) R. Nishiyabu, Y. Kubo, T. D. James and J. S. Fossey, *Chem. Commun.*, 2011, **47**, 1124–1150.

28 (*a*) S. H. Lim, L. Feng, J. W. Kemling, C. J. Musto and K. S. Suslick, *Nat. Chem.*, 2009, **1**, 562–567; (*b*) P. Anzenbacher Jr, P. Lubal, P. Buček, M. A. Palacios and M. E. Kozelkova, *Chem. Soc. Rev.*, 2010, **39**, 3954–3979; (*c*) J. J. Lavigne and E. V. Anslyn, *Angew. Chem., Int. Ed.*, 2001, **40**, 3118–3130.

